

## Mechanical testing of extruded magnesium for the development of automobile seat frame structures

S.P. Sikora<sup>1,\*</sup>, L. Bergmann<sup>2</sup>, E. Beeh<sup>1</sup>, H. Sulaiman<sup>3</sup>

<sup>1</sup> German Aerospace Center (DLR e.V.), Institute of Vehicle Concepts,  
Material and Process Applications for Road and Rail Vehicles, Stuttgart, GER.

<sup>2</sup> Helmholtz-Zentrum Geesthacht GmbH, Institute of Materials Research,  
Materials Mechanics, Solid-State Joining Processes, Geesthacht, GER.

<sup>3</sup> Faurecia Autositze GmbH, Seat Structure Systems Division,  
Advanced Manufacturing Engineering, Metal Forming, Stadthagen, GER.

\* Correspondence to: [sebastian.sikora@dlr.de](mailto:sebastian.sikora@dlr.de).

### Keywords

Magnesium alloy, ME21, extrusion, material characterization, closed profile, friction stir welding

### Abstract

To validate a novel structural concept in magnesium lightweighting in early development stages, a magnesium alloy of type MgMnCe is characterized at coupon level and validated at profile level. The feasibility of friction stir welding is confirmed to integrate the alloy into the structure.

Specimens are extracted from or set up on basis of generic profiles. For characterization amongst others, miniature tensile specimens in extrusion and transverse direction are utilized. Tensile results show the orthotropic material character of the ME21 alloy used. In transverse direction stiffness as well as strength increases, while elongation at break decreases. The material shows a strongly nonlinear, irreversible material behavior starting at small loads and a moderate strain-rate dependency.

On profile level, closed rectangular profiles in four-point bending are used for validation at high impact velocities. These tests reveal large deformation without local failure. This deformation makes the use of closed rectangular profiles promising for the application in seat backrest structures.

## 1 Introduction

In large-scale production of vehicle seats, high and ultra-high strength steel alloys prevail because of challenging requirements. The potentials of metal lightweight structures using steel and aluminum are exhausted to a large extent. The German national project FUMAS (Functionally Integrated Magnesium Lightweighting for Automobile Seat Structures) aims at weight reduction of a seat structure by using extruded magnesium and a novel process route in manufacturing. A concept for a lighter seat backrest structure is developed, dimensioned and evaluated. This predevelopment process is based on digital as well as experimental methods and is validated with generic substructures. The development process is finalized with an impact test on a prototypical seat structure. The partners of FUMAS are shown in Fig. 1.



Fig. 1: FUMAS project logo and consortium.

FUMAS uses a magnesium alloy of type MgMnCe in an extrusion process. The main alloy constituents are about 1.5 % manganese, 1 % rare earth elements (cerium and lanthanum), mainly being cerium. For simplicity, the material will be called ME21. Other similar ME21 alloys were examined earlier [1,2]. Here, the manganese proportion was higher at above 2 % and magnesium sheets were investigated, not applying the material in a structure.

In FUMAS, two concepts have been developed – a primary concept variant utilizing friction stir welding (FSW) and an alternative concept variant basing on injection adhesive bonding (IAB). This work will focus on the FSW concept, which is displayed in Fig. 2. The primary concept variant consists of an upper magnesium assembly and a bottom steel assembly. The 3-part magnesium frame structure contains a frame profile realized as formed extrusion profile with a thickness of 4 mm

and a pair of 2 mm thick surrounding support structures. The steel structure is a state-of-the-art welded assembly of two so called mobile gussets and the cross member. The shown Mg-Mg lap joint as well as the Mg-St lap joint are joined by means of FSW.

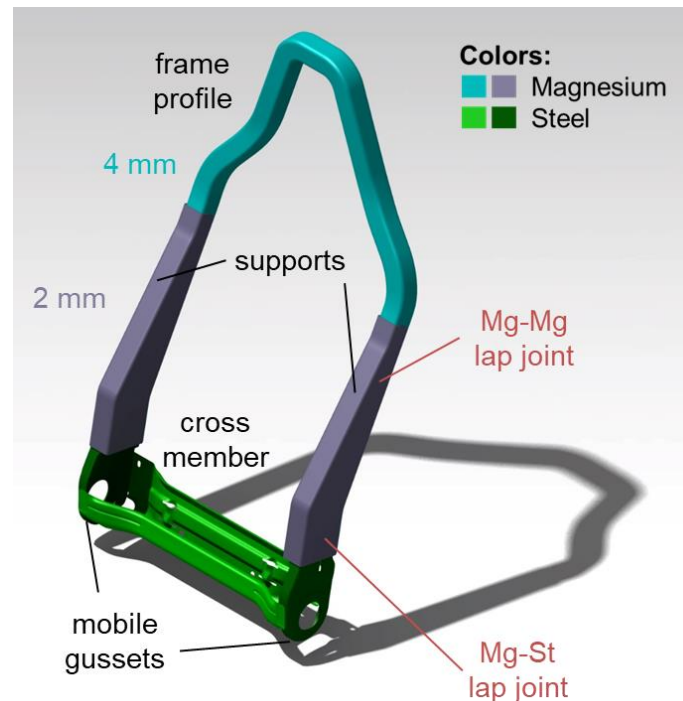


Fig. 2: Primary FUMAS concept for the seat backrest structure based on friction stir welding of a magnesium and a steel assembly.

The paper at hand presents fundamental experiments used in the development process of the structure. Experiments concerning the material, the structure and the joining technologies have been used. The ones that are mechanically essential for the solution design will be shown in the following chapters – starting with the characterization of the magnesium alloy at coupon level (chapter 2) and continuing to a validation on profile level (chapter 3). Main experimental studies concerning FSW feasibility for the integration of magnesium into the concept completes the main body of this work (chapter 4). Chapter 5 summarizes and concludes.

## 2 Characterization at coupon level

Based on an early version of the structure concept, generic extruded profiles (Fig. 3) were used to extract various coupon specimens – in extrusion direction (ED) and transverse direction (TD). This double chamber profile consists of closed rectangular chambers with wall thicknesses of 2 and 4 mm with a connection, which is 3 mm thick.

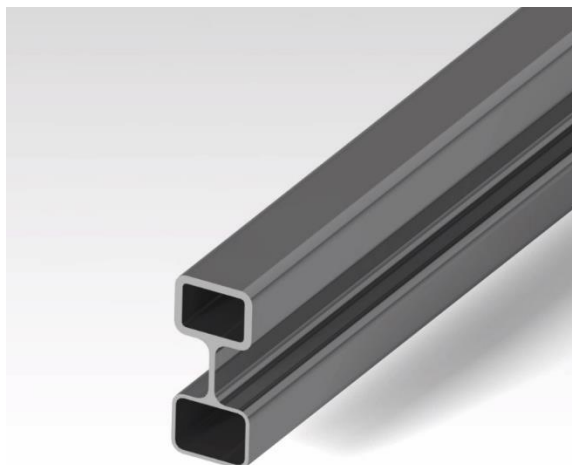


Fig. 3: Generic profiles used for diverse coupon extraction.

To start the characterization of the ME21 alloy, quasi-static tension and compression tests were conducted to evaluate orthotropy and tension-compression asymmetry of the material. The resulting representative engineering stress-strain curves are shown in Fig. 4, where relative displacements were optically determined with greyscale correlation in plane (2D). Standardized tensile tests close to DIN 50125 were used in extrusion direction, which revealed an ultimate strength of 205 MPa and a break elongation of 16 %. In transverse direction, a miniature specimen geometry was chosen to enable extraction from the lid of the rectangular profiles. Consequently, these miniature specimens have a total length of 28 mm, an optical gauge length of 4 mm measuring a rectangular cross section with a width of 3 mm. To prove validity of these specimens, first of all, tests in extrusion direction have been repeated with the miniature geometry. As shown in Fig. 4 and as desired, the results are the same as for standardized tests. Therefore, proceeding with the miniature specimens in transverse direction, a significant orthotropy is determined for ME21. The transverse ultimate tensile strength is 229 MPa and the elongation at break is 12.5 %. Also, the stiffness at small strains rises

significantly, compare Fig. 4. For compression tests, the test of Zhou et al. [3] is used. This testing method uses a single-sided groove in a supporting testing apparatus. Lateral support of the thin-walled coupon is required only at the back side of the specimen. This compression test yields the results in Fig. 4 in extrusion direction. Differences between tension and compression are significant. But at first glance, the difference of yield strength between tension and compression is smaller than known from other magnesium alloys like AZ31, compare studies of Zhou et al. [3,4]. This depends on the determination and definition of the yield strength.

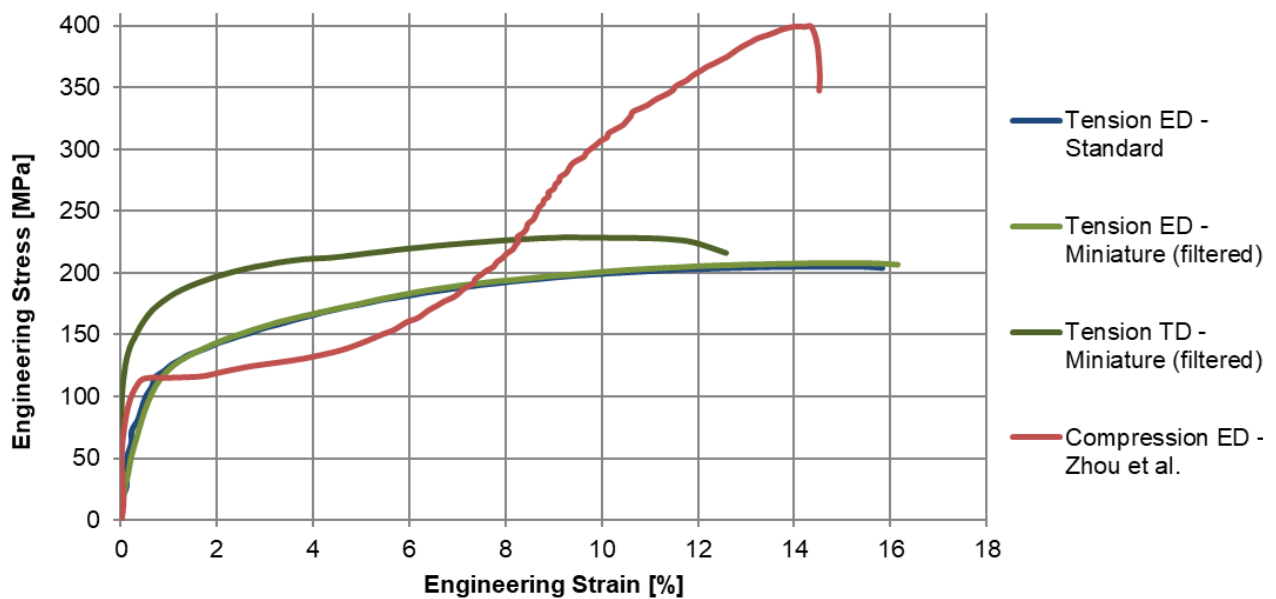


Fig. 4: Stress-strain curves in tension and compression for extrusion and transverse direction – orthotropy and tension-compression asymmetry of ME21. Coupon thickness 2 mm.

To investigate the material concerning elastic and plastic (or irreversible) deformation, cyclic quasi-static tensile tests with increasing load were conducted using strain gauges centrally applied on standardized specimens. At constant and equal loading and unloading traverse velocity, the specimen is loaded up to 20 MPa, unloaded, then loaded to 30 MPa, and so on every cycle increasing the load by 10 MPa. The results for a representative specimen are compiled in Fig. 5, where hysteresis loops become apparent for unloading and reloading processes. Starting at small loads already, a nonlinear stress-strain behavior is observed, considering the envelope of the curve, and remaining strains in the unloaded states are captured. The upper reversal points (reaching the defined load levels) and the lower reversal points in the unloaded states are used to determine

effective elastic moduli of the plastified material for all levels. These linear-elasticity magnitudes are also illustrated in Fig. 5. For deformation close to zero, i.e. small hysteresis loads, an effective modulus of about 44 GPa is determined, as expected for magnesium alloys. Then with increasing strain, the effective modulus drops to half of its original value (22 GPa), which denotes a significantly lower stiffness of the plastified material. In the application this means changing elastic properties when preloads, e.g. from misuse load cases, have affected the material. Revisiting the evaluation of the yield strength, the frequently used yield strength  $R_{p0.2}$  is also visualized in Fig. 5. It can be found close to 90 MPa, showing that a considerable nonlinearity is neglected using this characteristic. The material shows a strongly nonlinear, irreversible material behavior, which suggests the use of a low plastic limit to model it numerically.

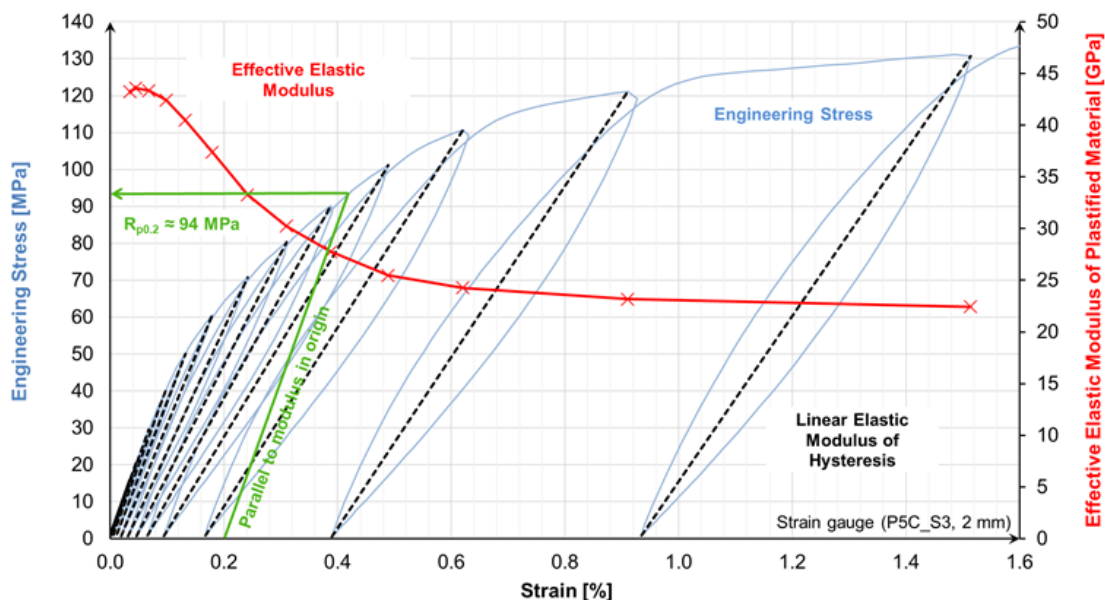


Fig. 5: Cyclic quasi-static tensile tests with increasing load – effective elastic stiffness.

In seat structure development, the most demanding load cases are crash load cases, in this case especially the rear impact. Therefore, coupon testing to determine the strain-rate sensitivity is crucial. Tensile tests according to DIN EN ISO 26203-2 were conducted. A specimen is shown in Fig. 6(a) and the results for representative specimens in Fig. 6(b) for a range of the piston velocity from 0.01 mm/s up to 1000 mm/s – thus covering five orders of magnitude. The results suggest that there is primarily a strain-rate dependency in the two lowest orders of magnitude (belonging to range from

0.01 to 1 mm/s piston velocity). Here, strength rises and elongation at break drops. From there to higher strain rates, only a slight increase of strength and elongation at break is observed.

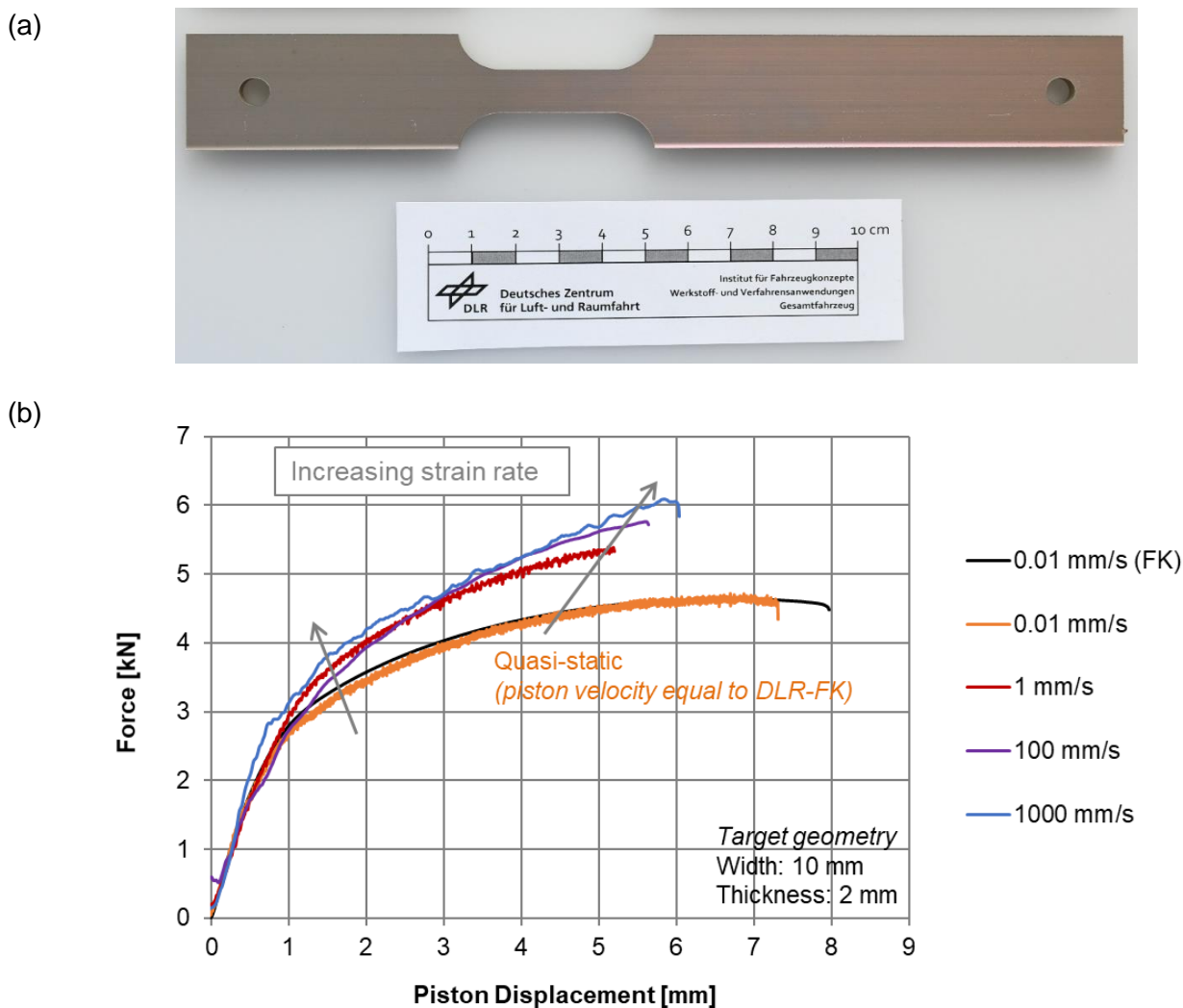


Fig. 6: Dynamic tensile tests: (a) Specimen, (b) Force-displacement curves for different piston velocities. The two different curves at 0.01 mm/s were measured using different machines: a quasi-static (at DLR-institute FK) and a high-velocity testing machine.

Beyond the presented tests, a big range of further aspects was experimentally covered. It may be emphasized that for all these studies, coupons have been cut from the profiles introduced in Fig. 3.

Further dependencies that were screened and studied are:

- Material thickness (2 mm / 4 mm): Nearly no change observed in tensile strength, but increased stiffness and elongation at break for 4 mm thickness.
- Profile instance: No systematic dependencies from profile detected.

- Position in profile (lid or sides, front / center / back): No dependency from extraction side, no changes along profile length found.
- Other stress states tested: Shear, shear tension, notched tension.

As a next step, the material application is validated using profiles.

### 3 Validation at profile level

One of the critical requirements in seat development is that the structure may not rupture locally in set crash situations. Many materials tend to embrittle at high strain rates, which is also the concern for magnesium structures. To experimentally study whether the design potentially can bear required loads, bending at high impact velocities was considered. In rear crash situations inertia pushes the passenger into the backrest rapidly resulting in bending of the seat structure with a load at the neck contact, compare Fig. 2. From there, the load has to be transferred into the body of the vehicle via the mobile and later the fixed gussets. The first abstraction level of one half of the backrest structure is a rectangular closed profile (single-chamber profile), which also can be extracted from the generic profile in Fig. 3. To comply with the length of a backrest structure, a length of 720 mm was chosen. The choice of four-point-bending, an outer rigid anvil distance of 600 mm and an inner one of 200 mm lead to the test setup as shown in Fig. 7(a). The chamber profiles have an outer rectangular shape of 40 mm in width and 30 mm in height. Here, the upper traverse is the fixed and the piston is the moving component. The inner rigid anvils as well as the inner 4-point bending adapter are attached to the piston that is driven by a hydraulic testing machine. Two force transducers are installed between the traverse and the frame of the machine. Fig. 7(a) shows an example of a situation after a test of a profile with 4 mm thickness. As desired, in this case no local rupture or other failure was observed. The tested profile exhibited large plastic deformation, which is considered as extremely good-natured behavior.

Fig. 7(b) shows force-displacement results for the two different wall thicknesses 2 and 4 mm for increasing piston velocities. The piston velocities range from 0.1 mm/s up to 10 m/s. At the maximum (36 km/h) this is the magnitude of impacts considered in seat development like required in UN/ECE-R17 or other regulations. Comparing the magnitude of the load at the same piston velocity, it is



recognizable that the load transfer increases disproportionately with the profile thickness. Doubling the thickness, almost leads to a tripling of the load transferred. This is due to the fact that with the chosen constraints (anvils) in the test, local failure can be observed for 2 mm thickness at anvil contact resulting in local buckling. Thus, for the chosen rectangular profile with 2 mm thickness the contact and load transfer is not designed appropriately. For 4 mm thickness this is the case and therefore smooth, good-natured deformation induced. This makes lightweighting using extruded magnesium promising for seat development, requiring a suitable design. Also, it has been shown that increasing strain rate does not lead to embrittlement.

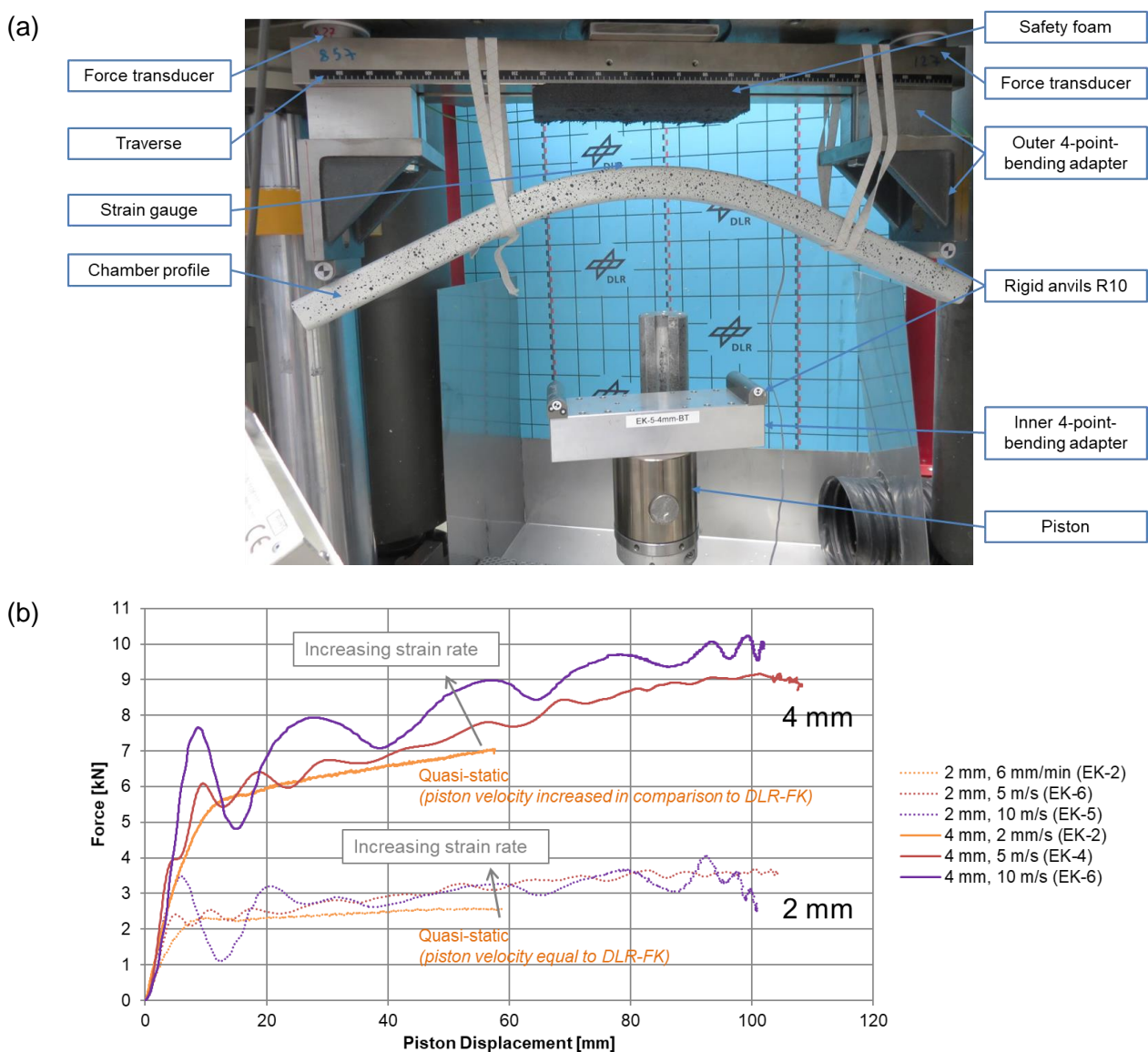


Fig. 7: Dynamic profile 4-point bending tests: (a) Test setup with deformed profile after test, (b) Force-displacement curves for different piston velocities for both wall thicknesses 2 and 4 mm. All results determined at the same high-velocity testing machine and filtered. Quasi-static tests stopped earlier than impact tests at high speeds, thus end of curve not comparable.

#### 4 Integration into concept with friction stir welding

In FUMAS, as primary joining technology friction stir welding (FSW) was pursued to integrate magnesium parts into the structure. The process was patented in 1991 by TWI in the UK and by now is mature to be used in large-series production. The main motivation for this welding process is to use an environmentally-friendly process (no additional material, or shielding gas). FSW is a solid-state joining process, i.e. the needed energy to perform the process is reached below the melting point of the base material, eliminating re-solidification problems and resulting in less distortion of the welded components. A further advantage of FSW is that due to the intensive mechanical work, during stirring of the material, there is a strong grain refinement in the stir zone (weld nugget), increasing the mechanical properties in the stir zone (SZ).

##### *ME21-ME21 in butt-joint configuration considering process and quality*

In order to develop proper FSW process parameters (rotational speed, welding speed, force) to weld ME21, a FSW tool with a scrolled shoulder and conical threaded probe with 2.75 mm length was used, shown in Fig. 8.

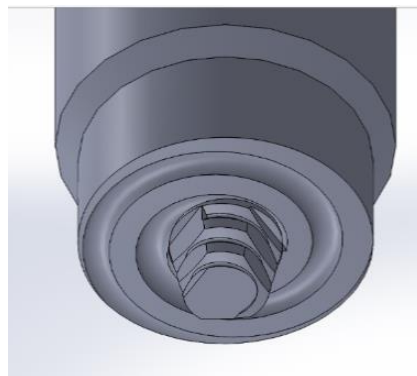


Fig. 8: FSW tool geometry.

In Fig. 9(a), an example ME21-ME21 butt-joint configuration joining the generic profile is shown. At the joint, the material thickness is 3 mm. A welding speed of 1.5 m/min was used. The resulting welding surface shows an excellent surface finishing – with no flash or underfill, compare Fig. 9(b). In Fig. 9(c), the cross section of the weld with the stir zone in the center is shown, which represents

the volume of the material subjected to severe mechanical work. This reduces the grain size in the SZ, as can be seen in the microstructure in Fig. 9(d).

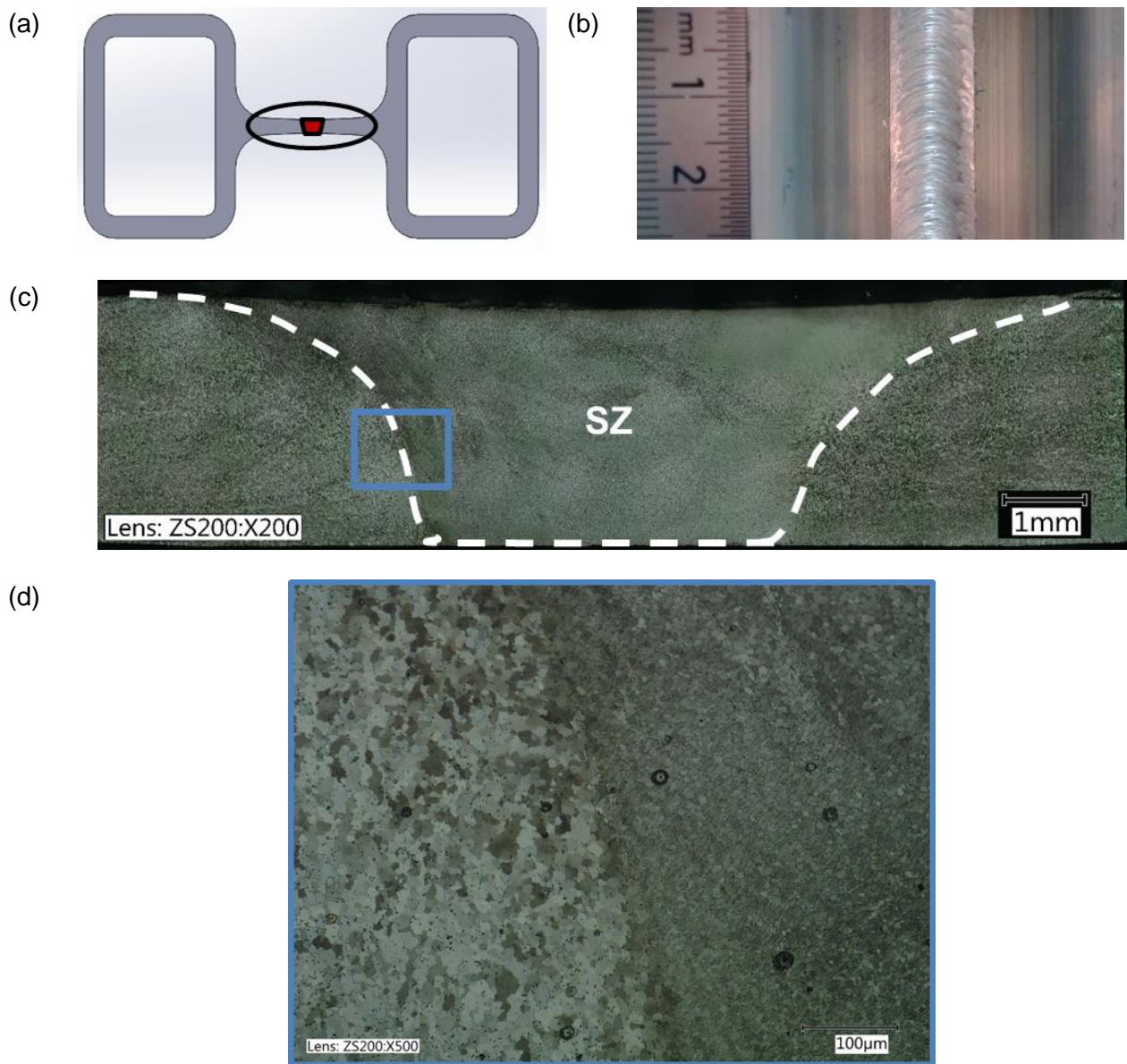


Fig. 9: FSW ME21-ME21 butt joint: (a) Configuration in generic profile, (b) Surface finishing, (c) Cross section, (d) Microstructural change in the transition zone.

In order to determine the mechanical properties, samples with 20 mm weld length (in depth direction of Fig. 9(a)) have been tested in quasi-static conditions achieving an ultimate tensile strength (UTS) of 110 MPa for the profile specimen. The failure occurred outside the weld at the curvature of the extruded profile, demonstrating that the weld is not the critical location for this butt-joint specimen.

*ME21-ME21 in butt- and lap-joint configuration considering process forces*

In case the stiffness of the profile is not sufficient to bear and transfer the FSW process forces, the profile collapses, deforms or reveals internal volumetric defects within the joint. Fig. 10(a) presents an example of a butt-joint configuration, in which the profile is locally being deformed by the tool producing a volumetric defect inside the joint. Fig. 10(b) shows a second example, where the supporting lower joining partner in a lap-joint configuration does not withstand the process forces completely. Therefore, some volumetric defects are observable. In this joint configuration the tool probe plunges through the upper material until inserted into the lower material between 0.5 mm up to 1 mm, joining both profile lids.

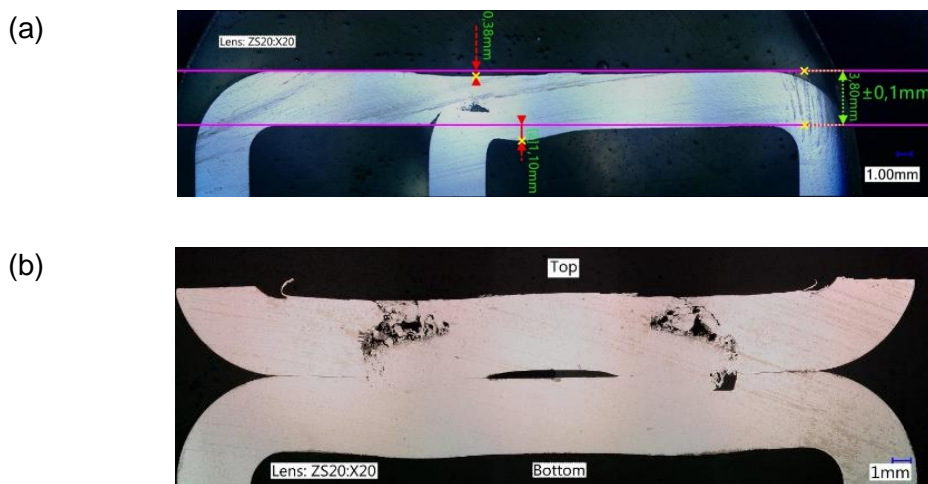


Fig. 10: Defects and deformation in FSW ME21-ME21 joints:  
 (a) Butt joint in modified generic profile joining lid and corner,  
 (b) Lap joint of generic profile lids.

*ME21-DP1000 in lap-joint configuration considering weldability*

In order to produce sound welds in an overlap-joint configuration, the softer material is typically positioned on the side where the tool is contacting first. There is no restriction for metallic material combinations [5]. Recently, developments in refill FSW at HZG show that it is also possible to weld polymers with metallic materials [6,7]. In the FUMAS magnesium-steel joint, there is no feasibility to position the steel material on the tool side. Considering the temperature to plasticize steel of around 900°C, far above the melting temperature of the magnesium, the materials cannot be stirred. With the FSW tool positioned on the magnesium side, the tool plunges through the magnesium scratching

the steel surface in order to activate the surface and get improved diffusion bonding. The mechanical anchoring is also increased due to the roughness created at the interface.

Welds were performed using 2 mm thick ME21 and 0.8 mm thick DP1000 with a welding speed of 500 mm/min and tool probe length of the magnesium base material thickness. The cross section shows the stir zone located in the magnesium and no deformation in the steel, compare Fig. 11.



Fig. 11: FSW ME21-DP1000 lap joint: Cross section.

In order to determine the mechanical properties of this joint type, single-lap tensile shear specimens 50 mm wide (corresponding to weld length) were cut and were quasi-statically tested. As a result, a UTS of 186 N per mm weld length was obtained.

Referring to Fig. 2, in the final seat backrest design Mg-Mg and Mg-St lap-joints are implemented, for which feasibility according to the shown studies is validated.

## 5 Conclusion

A large variety of experiments enabled the development of a seat backrest structure made of a magnesium alloy of type MgMnCe (ME21) using formed profiles. The key contents and conclusions of this paper are:

- The FUMAS seat frame concept uses an extruded magnesium alloy in a novel way, that has yet to be fully exploited.
- Experimental validation ranges from microstructure studies via chamber profiles to a prototypical linear impactor test of the seat structure.
- The magnesium alloy of type MgMnCe has been characterized extensively: It reveals an orthotropic, strongly nonlinear, moderately strain-rate dependent stress-strain behavior.
- Structural generic validation has been based on 4-point bending of chamber profiles demonstrating large ductile deformations, which are promising for seat development.
- Friction stir welding is applied to integrate magnesium into the concept considering process forces and weldability, focusing on lap-joint configuration. Welding speeds with industrial relevance have been determined.

## 6 Acknowledgments

The authors acknowledge the financial support by the German Federal Ministry for Economic Affairs and Energy (BMWi) through TÜV Rheinland Consulting GmbH. We thank our colleagues from the project FUMAS who provided insight and expertise that greatly assisted the research.

## 7 References

- [1] Gall, S., Coelho, R.S., Müller, S., Reimers, W.: Mechanical properties and forming behavior of extruded AZ31 and ME21 magnesium alloy sheets. *Materials Science & Engineering A* 579, 180–187 (2013)
- [2] Huppmann, M., Gall, S., Müller, S., Reimers, W.: Changes of the texture and the mechanical properties of the extruded Mg alloy ME21 as a function of the process parameters. *Materials Science and Engineering A* 528, 342–354 (2010)
- [3] Zhou, P., Beeh, E., Friedrich, H.E.: A Novel Testing Method for Uniaxial Compression of Thin-Sheet Magnesium Alloys. *Experimental Mechanics* 56, 513–519 (2016)
- [4] Zhou, P., Beeh, E., Friedrich, H.E.: Influence of Tension-Compression Asymmetry on the Mechanical Behavior of AZ31B Magnesium Alloy Sheets in Bending. *Journal of Materials Engineering and Performance, JMEPEG* 25, 853–865 (2016)
- [5] Suhuddin, U.F.H., Fischer, V., Kostka, A., dos Santos, J.F.: Microstructure evolution in refill friction stir spot weld of a dissimilar Al–Mg alloy to Zn-coated steel. *Science and Technology of Welding and Joining* 22:8, 658-665 (2017)
- [6] André, N.M., Goushegir, S.M., Scharnagl, N., dos Santos, J.F., Canto, L.B., Amancio-Filho, S.T.: Composite surface pre-treatments: Improvement on adhesion mechanisms and mechanical performance of metal-composite friction spot joints with additional film interlayer. *Journal of Adhesion* 94:9, 723-742 (2018)
- [7] André, N.M., dos Santos, J.F., Amancio-Filho, S.T.: Evaluation of Joint Formation and Mechanical Performance of the AA7075-T6/CFRP Spot Joints Produced by Frictional Heat. *Materials*, 12, 891 (2019)